

Aquatic and Soil CO₂ Emissions from forested wetlands of Congo's Cuvette Centrale

Antoine de Clippele^{1*}, Astrid C. H. Jaeger^{1*}, Simon Baumgartner^{2,3}, Marijn Bauters⁴, Pascal Boeckx⁵, Clement Botefa⁶, Glenn Bush⁷, Jessica Carilli¹, Travis W. Drake¹, Christian Ekamba⁸, Gode Lompoko⁶,
5 Nivens Bey Mukwiele⁶, Kristof Van Oost³, Roland A. Werner¹, Joseph Zambo⁷, Johan Six¹, Matti Barthel¹

1 Department of Environmental Systems Science, ETH Zurich, Switzerland

2 Research Division Agroecology and Environment, Agroscope, Zurich, Switzerland

3 Earth and Life Institute, Université Catholique de Louvain, Louvain-la-Neuve, Belgium

10 4 Q-ForestLab, Department of Environment, Ghent University, Belgium

5 Isotope Bioscience Laboratory, Department of Green Chemistry and Technology, Ghent University, Belgium

6 ICCN Jardin de Botanique d'Eala, Mbandaka, Democratic Republic of Congo

7 Woodwell Climate Research Center, USA

8 Coordination Provinciale de l'environnement, Mbandaka, Democratic Republic of Congo

15 *These authors contributed equally to this study.

Correspondence to : Antoine de Clippele (antoine.declippele@usys.ethz.ch)

Abstract. Within tropical forest ecosystems, wetlands such as swamp forests are an important interface between the terrestrial and aquatic landscape. Despite this assumed importance, there is a paucity of carbon flux data from wetlands in tropical Africa.
20 Therefore, the magnitude and source of carbon dioxide (CO₂) fluxes, carbon isotopic ratios, and environmental conditions were measured for three years between 2019 to 2022 in a seasonally flooded forest and a perennially flooded forest in the *Cuvette Centrale* of the Congo Basin. The mean surface fluxes for the seasonally flooded site and the perennially flooded site were $2.36 \pm 0.51 \mu\text{mol m}^{-2} \text{s}^{-1}$ and $4.38 \pm 0.64 \mu\text{mol m}^{-2} \text{s}^{-1}$ respectively. The time series data revealed no marked seasonal pattern in CO₂ fluxes. As for the environmental drivers, the fluxes at the seasonally flooded site exhibited a positive correlation with
25 soil temperature and soil moisture. Additionally, the water level appeared to be a significant factor, demonstrating a quadratic relationship with the soil fluxes at the seasonally flooded site. $\delta^{13}\text{C}$ values showed a progressive increase across the carbon pools, from above-ground biomass, then leaf litter, to soil organic carbon (SOC). However, there was no significant difference in $\delta^{13}\text{C}$ enrichment between SOC and soil respired CO₂. This lack of enrichment can be attributed to either a significant contribution from the autotrophic component of soil respiration or a result of closed system dynamics.
30 An *in-situ* derived gas transfer velocity ($k_{600} = 2.95 \text{ cm h}^{-1}$) was used to calculate the aquatic CO₂ fluxes at the perennially flooded site. Despite the low k_{600} , relatively high CO₂ surface fluxes were found due to very high partial pressure of CO₂ (pCO₂) values measured in the flooding waters. Overall, these results offer a quantification of the CO₂ fluxes from forested wetlands and provide an insight of the temporal variability of these fluxes as well as their sensitivity to environmental drivers.

1 Introduction

35 Along with the oceans and Northern Hemisphere forests, tropical forests represent one of the three main components of the
global carbon sink (Mitchard, 2018). However, due to relatively high gross primary productivity, temperature and soil
moisture, tropical forest soils also constitute a large terrestrial source of carbon dioxide (CO₂). Indeed, tropical regions are
estimated to contribute up to 64% of global soil respiration, rendering it as the largest flux of CO₂ from terrestrial ecosystems
to the atmosphere (Hashimoto et al., 2015; Huang et al., 2020).

40

Wetland cover in the tropical Congo Basin is estimated to range between 332,620 and 359,556 km² (Bwangoy et al. 2010;
Fatras et al. 2021). This area includes the *Cuvette Centrale*, which spans approximately 167,600 km² and hosts lowland and
swamp forests, including the largest peatland complex across the tropics (Crezee et al., 2022). With catchment drainage from
north and south of the equator as well as sustained rainfall at the center of the basin (Breitengroß, 1972; Runge, 2007), the
45 *Cuvette Centrale* shows near permanent inundation. Characterizing CO₂ fluxes in this extensive region is especially important
since inland waters are increasingly recognized as significant sources of greenhouse gases (GHG) within the terrestrial
landscape (Bastviken et al. 2011; Drake, Raymond, and Spencer 2018; Borges, Darchambeau, et al. 2015; Rosentreter et al.
2021) and notably in global carbon dioxide emissions (Raymond et al. 2013). Recent data additionally suggests that the Congo
Basin's inland waters might emit more carbon (C) per area than their counterparts in the Amazon Basin (Alsdorf et al., 2016).
50 Profound hydrological (Alsdorf et al., 2016), structural (Lewis et al., 2013), ecological (Parmentier et al., 2007; Slik et al.,
2015), aquatic biogeochemical (Borges et al. 2015), and terrestrial biogeochemical (Hubau et al., 2020) differences indicate
that GHG flux estimates cannot simply be transferred from the Neotropics to the Afro-tropics. However, while recent research
on GHG emission from the Congo Basin has focused on either riverine (Borges et al., 2019; Bouillon et al., 2012; Mann et al.,
2014a; Upstill-Goddard et al., 2017) or terrestrial fluxes (Baumgartner et al. 2020; Gallarotti et al. 2021; Barthel et al. 2022;
55 Daelman et al. 2024), direct measurements from forested wetlands are still lacking. Despite its immense global importance,
only two studies, to the best of our knowledge, have been looking into GHG emissions from Congo's wetlands (Tathly et al.
1992; Barthel et al. 2022).

Forested wetlands/swamp forests are located at the transition zone between the terrestrial and the aquatic realm. The duration
60 and seasonality of the flooding in the forests will constrain the contribution from/to the river system. While flooded, the swamp
forests are connected to the river system and receive and/or discharge materials from/to the river network (Aufdenkampe et
al., 2011). Variations of riverine greenhouse gas concentrations have been shown to be driven by fluvial-wetland connectivity
for the *Cuvette Centrale* based on data from 10 expeditions across the Congo River network (Borges et al., 2019). Furthermore,
streams and rivers draining Congo's flooded forests were found to have the highest dissolved concentrations of CO₂ among
65 different land cover types in the Basin, indicating the substantial contribution of forested wetlands on the overall inland water
GHG budget (Mann et al., 2014b).

Here, we report three years of carbon dioxide (CO₂) fluxes measured from two sites situated within the *Cuvette Centrale*: a seasonally flooded forest site and a perennially flooded forest site. During the observation period, surface CO₂ fluxes whether soil or aquatic, were measured fortnightly to capture the seasonal and inter-annual variation of the fluxes. Hence, these results provide insights into the temporal dynamics of CO₂ fluxes in forested wetlands across two different flooding regimes.

2 Materials and Methods

2.1 Study sites

The sites were located near the town of Mbandaka (Democratic Republic of the Congo, Équateur province), which is located at the Ruki-Congo confluence within the *Cuvette Centrale* (Figure 2). The mean annual precipitation and mean annual temperature of the sampling area are 1588 mm and 25 °C, respectively (see the measurements detailed below). The long dry season in Mbandaka typically lasts from July to August, while the short dry season occurs between January and February. Here, surface CO₂ fluxes were measured at two different sites across two different hydrological regimes, one in a seasonally flooded forest (N 0.06335, E 18.31054, 300 m a.s.l.) – referred to as SFF site – and in a perennially flooded forest (S 0.03135, E 18.3102, 305 m a.s.l.) – referred to as PFF site (Figure 1).

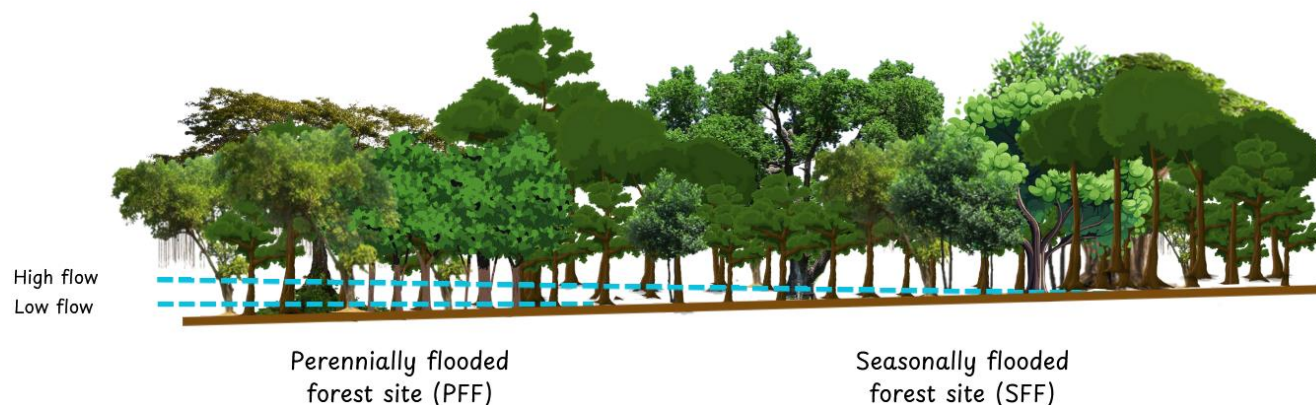


Figure 1. Diagram showing the location of the two experimental sites (PFF and SFF) relative to the hydrological gradient.

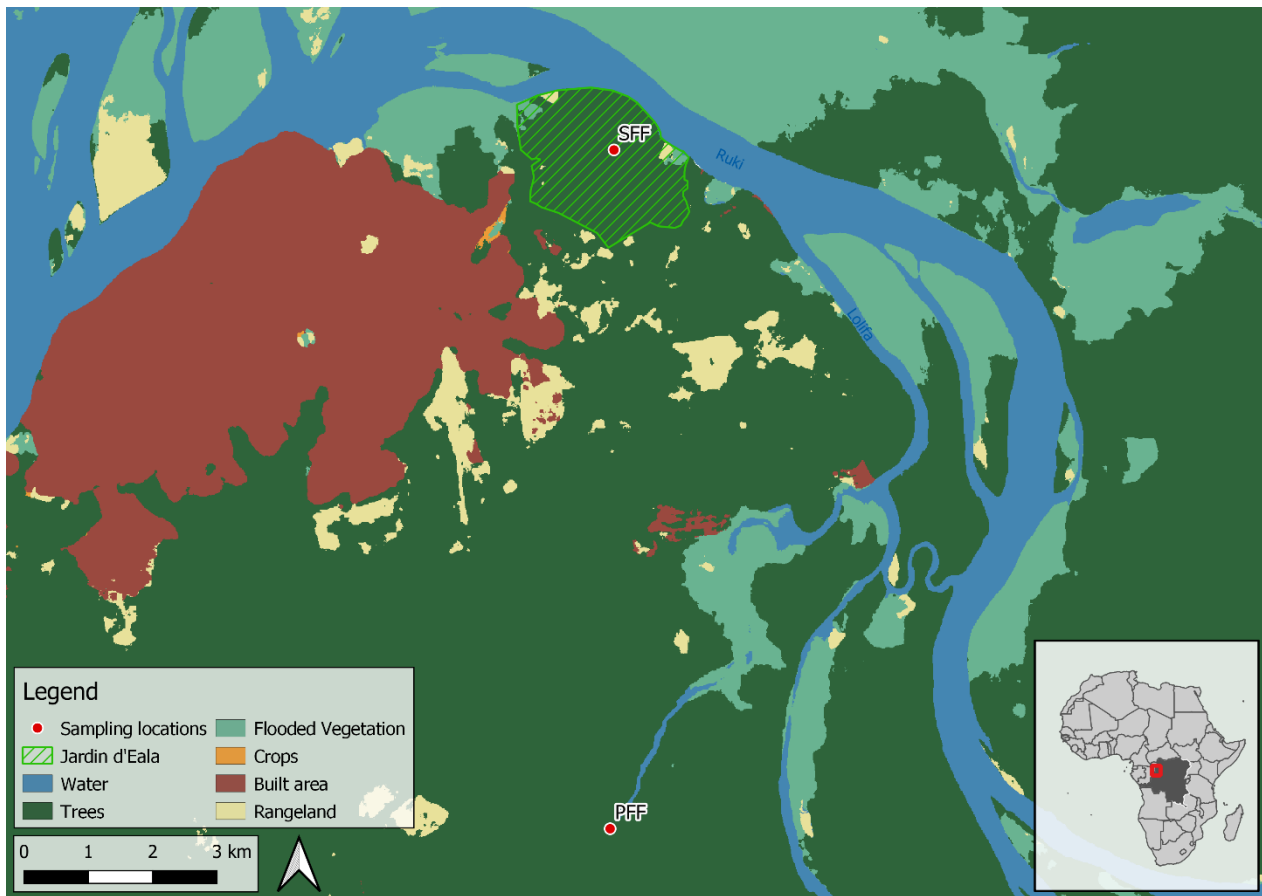
The seasonally flooded forest site (SFF) investigated was located within a botanical garden 7 km from the center of Mbandaka (*Jardin Botanique d'Eala*, operated by the *Institute Congolais pour la Conservation de la Nature* (ICCN)). The botanical garden comprises 371 ha of land consisting of 35% dense swamp forest, 14% forest on firm ground, 32% open forest, and the remaining area consisting of secondary forest, grassland, and deforested land, of which 189 ha are protected forest area. There are 3500 different trees and herbaceous plant species, with the main tree species being *Hevea brasiliensis*, *Ouratea arnoldiana*, *Pentaclethra eetveldeana*, *Strombosia tetandra*, and *Daniella pynaertii*. The soil at the site, covered by a thick litter layer, was characterized as Eutric Gleysols (texture 42/50/8 sand/silt/clay in %, bulk density 1.27 g cm⁻³). The litter layer harbors a dense

90 mesh of fine roots, whereas almost no roots were found to penetrate the upper mineral soil layer (0-30 cm). The SFF site is seasonally flooded from about December to January (~2 months).

At the SFF site, combined soil moisture and temperature sensors (ECH₂O 5TM, Meter Group, Inc. USA) connected to loggers (Em50, Meter Group, Inc., USA) were installed at 10 and 30 cm depth, respectively. The data was recorded every 6 h.
95 Unfortunately, one logger was stolen and the other logger stopped working during deployment; thus, data is only available from November 2019 to July 2020 (Figure 3). Afterward, TMS-4 dataloggers (TOMST, Czechia) were installed in December 2020 to record surface volumetric soil water content (0-14cm) and soil temperature at 8 cm depth in 15-minute intervals. Raw data (soil moisture count) retrieved from TMS-4 dataloggers was converted into soil VWC with calibrations curves, following Wild et al. (2019), using site-specific soil properties (soil texture: 42/50/8 sand/silt/clay in %, bulk density 1.27 g cm⁻³) and
100 measured soil temperatures. The soil VWC values from the ECH₂O 5TM sensors showed a systematic offset compared to those obtained from the TMS-4 dataloggers. This was attributed to instrument artefact and corrected by using the difference between maximum values. Furthermore, precipitation, air temperature, relative humidity, solar radiation, and wind speed data were retrieved for the observation period from the Trans-African Hydro-Meteorological Monitoring Observatory (TAHMO) station located in close vicinity to the forest site (ATMOS 41, Meter Group, Inc., USA).

105

The perennially flooded forest (PFF) site is located about 8 km upstream of the Congo-Ruki confluence, following a small side tributary named Lolifa. The headwater stream area is completely flooded for most of the year, making the stream bed channel indistinguishable. This creates a continuous wetland area where the PFF site is located. While the water is mostly stagnant at the site, a small drainage flow appears during the dry season (late June to early September). The site was accessed
110 with a motorized dugout canoe, and sampling was done fortnightly from the side of the canoe. The main tree species at the PFF site were *Uapaca sp*, *Irvigia smitii*, and *Daniella pynaertii* De Wild. Additional to the surface CO₂ fluxes, water samples were collected on the same day to measure pH, dissolved organic carbon (DOC) and total dissolved nitrogen (TDN). The presented C:N ratio was thus calculated using TDN rather than dissolved organic nitrogen (DON). Previous analyses (Drake et al., 2023) showed that TDN consistently comprised an average of 90% of DON and thus reflected well the relative changes
115 of DON concentrations. The specific methods used for sample processing and analysis as well as the calculations are described in Drake et al., (2023).



120 **Figure 2. Map presenting the two sampling sites in the vicinity of Mbandaka (Democratic Republic of the Congo). The boundaries of the Jardin botanique d'Eala are highlighted. Map data: © 2020-2023 Impact Observatory, Inc. and GADM.**

2.2 CO₂ fluxes

2.2.1 CO₂ surface fluxes at the SFF site

A total of six polyvinylchloride soil flux chambers (height = 0.3m, diameter = 0.3m) were installed in November 2019 at the SFF site. The SFF site was chosen as a representative site of the surrounding forest. The six chambers were spaced about 20 meters apart, randomly distributed across the site but accounting for variations in local microtopography. The chamber bases were inserted approximately 5 cm into the ground and remained in place throughout the measurement period, with the chambers left open except during sampling. Chambers affected by seasonal flooding were measured for as long they were not completely submerged at which point floating chambers (V = 17L) were used instead. Sampling with the soil chambers was conducted fortnightly for three consecutive years (2019/11 – 2022/12), totalling 403 flux measurements. Sampling was interrupted once for about six months due to logistical constraints (first half of 2022).

Each chamber lid was equipped with a thermocouple to measure headspace temperature, a vent tube to avoid pressure changes, and a sampling port. The sampling port had a 3-way Luer valve attached, connecting the syringe, needle, and chamber. Before withdrawing each gas sample from the headspace, chamber air was mixed by moving the syringe plunger several times; for soil GHG flux determination, gas samples were taken at timesteps of 20 min throughout 1 hour (t1 = 0 min, t2 = 20 min, t3 = 40 min, t4 = 60 min). A longer chamber closure time than recommended (Pavelka et al., 2018) was used to obtain robust Keeling plots along with the flux measurements. At each timestep, 20 mL of gas sample were stored in 12 mL pre-evacuated vials (Labco, UK) using a gas-tight disposable plastic syringe (20 mL). The resulting vial overpressure prevents air ingress due to temperature and pressure changes potentially occurring during transport and is required for sample withdrawal by the GC autosampler. To aid vacuum and sample preservation, each evacuated vial was sealed with an additional silicone layer (Dow Corning 734, Dow Silicones Corporation, USA). Soil CO₂ fluxes were calculated via linear concentration increase over time using the ideal gas law $PV = nRT$:

$$n = \frac{PV}{RT} \quad (1) \text{ and } F = \frac{\Delta n}{\Delta t} S^{-1} \quad (2)$$

with n moles of gas [mol], P partial pressure of trace gas [atm $\mu\text{mol mol}^{-1}$], R gas constant 0.08206 [L atm K⁻¹ mol⁻¹], T headspace temperature [K], F flux of gas [$\mu\text{mol m}^{-2} \text{s}^{-1}$], $\frac{\Delta n}{\Delta t}$ rate of change in concentration [mol s⁻¹], V chamber volume [L], and S surface area enclosed by chamber [m²]. The coefficient of determination (r^2) for the linear regression of CO₂ yielded a $r^2 > 0.95$ for 95% of the data (Supp. Fig. 1). All data with $r^2 > 0.1$ was kept for the statistical analyses. Such a low r^2 threshold was maintained because fluxes with low r^2 values are typically related to low flux rates rather than due to methodological or technical issues. Increasing the threshold would introduce a bias toward higher fluxes in the data.

2.2.2 Aquatic surface fluxes at the PFF site

The aquatic surface flux to the atmosphere (F_{CO_2} , $\mu\text{mol m}^{-2} \text{s}^{-1}$) from the PFF site was estimated according to a simple gas transfer model (Mann et al. 2014):

$$F_{\text{CO}_2} = k_x \cdot K_H \cdot (p\text{CO}_{2w} - p\text{CO}_{2a}) \quad (3)$$

where k_x is the freshwater gas transfer velocity of CO₂ [m s⁻¹], K_H is the Henry's constant for CO₂ [mol m⁻³ atm⁻¹], $p\text{CO}_{2w,a}$ the partial pressure of CO₂ in water and atmosphere, respectively [μatm].

Since the magnitude of the gas transfer velocity is governed by numerous factors (e.g., wind speed, water current velocity, slope), an *in-situ* gas transfer velocity k was calculated as 3.5 cm h⁻¹ using the aquatic fluxes from the SFF site sampled between 2022-07 to 2022-12 with the above-mentioned floating chamber ($V = 17$ L) and the corresponding dissolved CO₂ concentrations of the inundation water at the same site. The value of 3.5 cm h⁻¹ was then applied to the perennially flooded

forest dataset where no floating chamber measurements existed. Hence, fluxes from the PFF site were derived using the
165 measured gas transfer velocity from the SFF site (3.5 cm h^{-1}).

In order to compare the *in-situ* derived velocity k_x with the temperature normalized transfer velocity (k_{600}) for tropical wetlands
of 2.4 cm h^{-1} (Aufdenkampe et al., 2011), we used the equation from Pelletier et al. (2014) to convert k_x to k_{600} .

$$k_x = k_{600} \left(\frac{S_c}{600} \right)^{-b} \quad (4)$$

170

Where S_c is the gas specific Schmid number and b derived from literature (0.66 for wind speed $\leq 3 \text{ m/s}$; Pelletier et al. 2014).
The gas specific Schmid number is a function of water temperature (T in $^{\circ}\text{C}$) as defined by Wanninkhof (2014):

$$S_{cCO_2} = 1923.6 - 125.06T + 4.3773T^2 - 0.085681T^3 + 0.00070284T^4 \quad (5)$$

175

For pCO_{2a} , the tropospheric mean value from the year 2020 ($400 \mu\text{atm}$) was used while pCO_{2w} was determined using the
headspace equilibration technique. That is, 6 mL of bubble-free water sample were injected with a syringe into a 12 mL N_2 -
pre-flushed vial (Exetainer®, Labco, UK) pre-poisoned with 50 μL of 50% $ZnCl_2$ to stop the microbial activity. After sufficient
equilibration time, the remaining headspace was analysed for CO_2 concentrations using a gas chromatograph (see Section
180 below), and total dissolved concentrations were calculated based on Henry's law (see a detailed method in Supplementary).
For each date, pCO_{2w} samples were taken in triplicate with an average coefficient of variation (CV) of 8%.

2.3 Gas Chromatography

Gas samples were analyzed at ETH Zurich using a gas chromatograph (GC; Bruker, 456-GC, Scion Instruments, Livingston,
UK) separating CO_2 from residual air. After separation, the concentration of CO_2 was measured on a thermal conductivity
185 detector. GC calibration was done with a suite of three standards (Carbagas AG, Switzerland; PanGas AG, Switzerland) across
a concentration range from 249 to 3040 ppm CO_2 . Each standard was analysed ten times at start, middle, and end of each set
of 140-180 samples. Moreover, because of occasional high CO_2 sample concentrations, an entire system flush was done
between each sample measurement to avoid any carry-over effects. The same GC setup was used for both flux samples and
dissolved CO_2 samples.

190 2.4 $\delta^{13}\text{C}$ of soil-derived CO_2 fluxes and dissolved CO_2

The carbon isotopic composition of the CO_2 samples was analysed for one SFF CO_2 flux sample set of each month. That is,
after CO_2 concentration measurement with the GC, the same samples were analysed for $\delta^{13}\text{C}$ of CO_2 with a modified Gasbench
II periphery (Finnigan MAT, Bremen, D) coupled to an isotope ratio mass spectrometer (IRMS; Delta^{plus}XP; Finnigan MAT)
as described in Baumgartner et al. (2020). Post-run off-line calculation and drift correction for assigning the final $\delta^{13}\text{C}$ values

195 on the Vienna Peedee Belemnite (V-PDB) scale was done following the 'IT principle' (Werner and Brand, 2001). The $\delta^{13}\text{C}$ -
values of the laboratory air standards were determined at the Max-Planck-Institute for Biogeochemistry (Jena, Germany),
according to Werner, Rothe, and Brand (2001). The final soil CO_2 - $\delta^{13}\text{C}$ values were calculated using the Keeling plot approach
(Keeling, 1958) (Supp. Fig. 2).

200 $\delta^{13}\text{C}$ of dissolved riverine CO_2 was determined using the headspace equilibration technique as described in section 2.2.2.
Instead of concentration, $\delta^{13}\text{C}$ of the headspace was analysed via IRMS as described above. Samples were taken each month
from the Ruki river between 10-2022 to 06-2023 with 2-3 replicates per sampling (Supp. Fig. 4).

2.5 $\delta^{13}\text{C}$ of leaves, litter, and soils

Fresh leaf samples were taken from a range of the most representative tree species at two different timepoints (2019-11; 2023-
205 11). In addition, litter samples were collected at the same time and both were used to analyze the carbon isotopic composition
($\delta^{13}\text{C}$). Before analysis samples were dried, homogenized, and ground. Soil samples were taken in 2019-11, 2020-02 and 2023-
11 at 0-30 cm depth and air dried, sieved, and milled. All samples were analyzed using an elemental analyzer (Flash EA 1112
Series, Thermo Italy, former CE Instruments, Rhodano, Italy), interfaced with an IRMS (Finnigan MAT Delta^{plus} XP, Bremen,
Germany) via a 6-port valve (Brooks et al., 2003) and a ConFlo III (Werner et al. 1999). Soil samples are subsequently referred
210 to as soil organic carbon (SOC) samples. Calibration of laboratory standards (acetanilide, caffeine, tyrosine) was done by
comparison to the corresponding international reference materials provided by the IAEA (Vienna, Austria).

2.6 Water level

Direct measurements of the water level were not available for the whole observation period. Previous work showed a linear
relationship between the water level of the Congo River and the Ruki river (unpublished, Supp. Fig. 3). Additionally, the
215 rainfall and/or the hydrological dynamics of the river influence the water levels in the wetlands. In the *Cuvette Centrale*,
Georgiou et al. (2023) determined that the water levels of riverine locations in the Democratic Republic of the Congo (DRC)
correlate more with the hydrological dynamics of the river system than with the rainfall input. Hence, available daily
measurements of the water level of the Congo River in Mbandaka were used as a proxy of the water level below- and
aboveground at the SFF site. (Supp. Fig. 6). This data was extracted from an almost continuous record of water gauge readings,
220 collected in vicinity of the SFF site (~4 km) by the Congolese public institution, *Régie des Voies Fluviales*, since 1913.

2.7 Statistical Analyses

Daily environmental conditions were used to explain variability in the measured soil CO_2 fluxes ($n = 403$) at the SFF site. For
this, a linear mixed effects model was fitted using soil temperature, volumetric soil water content, and river level as fixed
effects. River level showed a non-linear relationship with surface fluxes. Hence, a quadratic term was added to account for the

225 non-linear effect. The predictor variables were standardized before fitting the models. All models controlled for repeated measurements in the same chambers, by adding chamber ID as a random intercept. Models were fitted by the restricted maximum likelihood method using *lme4* (Bates et al., 2015). Full and reduced models were compared using likelihood ratio test and adjusted r^2 values using *MuMin* package (Barton, 2020). Furthermore, a backward stepwise regression analysis was conducted on the full model, incorporating all effects and interaction terms, to identify the most parsimonious model with
 230 highest explanatory power (Kuznetsova et al., 2017). The resulting model included an additional interaction term between soil moisture and river level. However, this term was subsequently removed due to multicollinearity and its lack of practical significance. Marginal and conditional r^2 values for mixed effects were calculated using Nakagawa et al., (2017), inclusive r^2 estimated with partR2 package (Stoffel et al., 2021) and p-values using Satterthwaite's approximation with the *lmerTest* package (Kuznetsova et al., 2017). Additionally, confidence intervals for the effect estimates were computed to confirm the
 235 interpretation of the estimated parameters. The assumptions of the model were validated by verifying the linearity, normality and homoscedasticity of the residuals. Multicollinearity between the predictor variables was also estimated (Variance Inflation Factor (VIF) inferior to 3). Statistical differences between $\delta^{13}\text{C}$ values measured across the different carbon pools were tested with the Kruskal-Wallis test, followed by a pairwise Wilcoxon comparisons. Significance was established when the Bonferroni adjusted p-values were inferior to 0.05. Statistical and graphical data analysis were done in R v.4.3.2 (R Core Team, 2023) via
 240 RStudio v.2023.12.0 (RStudio Team, 2023), using the packages *tidyverse* v.2.0.0, *tydr* v1.3.0, *dplyr* v.1.1.4 (Wickham et al., 2023), *ggplot2* v. 3.4.4 (Wickham, 2009), *sjPlot* (Lüdecke, 2013) and *lubridate* v.1.9.3 (Grolemund and Wickham, 2011). QGIS version 3.16 was used to compile the map of the sampling locations.

3 Results

3.1 Environmental Conditions

245 The long dry season in Mbandaka is considered from July to August whereas the short dry season spans between January and February. However, frequent rainfall as shown in Figure 3 renders the region as relatively wet throughout the entire year. Annual precipitation was the highest in 2020 with 1855 mm and lowest in 2022 with 1417 mm (self-measured; Figure 3). The flooding period at the study site is typically centered around December and January. The highest weekly precipitation occurred in July and September of each year with 120 – 182 mm (Figure 3A). Overall, the weekly precipitation ranged from 0 – 182
 250 mm, with a monthly average of 31mm (Figure 3A).

Volumetric soil water content, hereinafter referred to as soil moisture, averaged $0.60 \pm 0.09 \text{ m}^3 \text{ m}^{-3}$, ranging between 0.35 to $0.76 \text{ m}^3 \text{ m}^{-3}$ for the observation period (Figure 3A). In general, the soil moisture showed strong seasonality, with an increase in November and peak values observed in January. Thereafter, the soil moisture decreased before stabilizing until the following
 255 wet season. This pattern was less pronounced over the 2021-2022 season (Figure 3A).

Soil and air temperatures were stable throughout the observation period (Figure 3B). Recorded mean air temperature at the weather station was 25.0 °C (± 0.7 °C), and mean soil temperature at the SFF site was 24.7 °C (± 0.3 °C) for the observation period.

260 3.2 Soil and aquatic CO₂ fluxes

Over the observation period, CO₂ fluxes from the PFF site were higher than from the SFF site (Figure 3F). At both sites, CO₂ fluxes exhibited intra-annual variability. However, distinct seasonal patterns were not clear. Notably, at the SFF site, the onset of flooding appeared to induce a decline in fluxes. Furthermore, among the environmental variables, CO₂ fluxes exhibited significant correlations with soil moisture, soil temperature, and river level (Table 1). At the PFF site, the highest fluxes were
265 recorded in June and August of 2020 with 5.71 and 5.76 $\mu\text{mol m}^{-2} \text{s}^{-1}$, whereas the lowest values were observed in September and October 2020 with 3.35 and 3.42 $\mu\text{mol m}^{-2} \text{s}^{-1}$. Mean weekly surface fluxes (F_{CO_2}) from the PFF site ranged from 3.35 to 5.76 $\mu\text{mol m}^{-2} \text{s}^{-1}$ with an average flux of $4.38 \pm 0.64 \mu\text{mol m}^{-2} \text{s}^{-1}$ using the *in-situ* derived gas transfer velocity of 3.5 cm h^{-1} (Figure 3E). Mean weekly surface fluxes (F_{CO_2}) from the SFF site ranged from 0.87 to 3.64 $\mu\text{mol m}^{-2} \text{s}^{-1}$ with an average of $2.36 \pm 0.51 \mu\text{mol m}^{-2} \text{s}^{-1}$. Here, the lowest flux was observed in July 2022 with 0.87 $\mu\text{mol m}^{-2} \text{s}^{-1}$, period corresponding to the
270 lowest soil moisture recorded (0.35 $\text{m}^3 \text{m}^{-3}$), while peaking in May 2020 with 3.64 $\mu\text{mol m}^{-2} \text{s}^{-1}$ (Figure 3E).

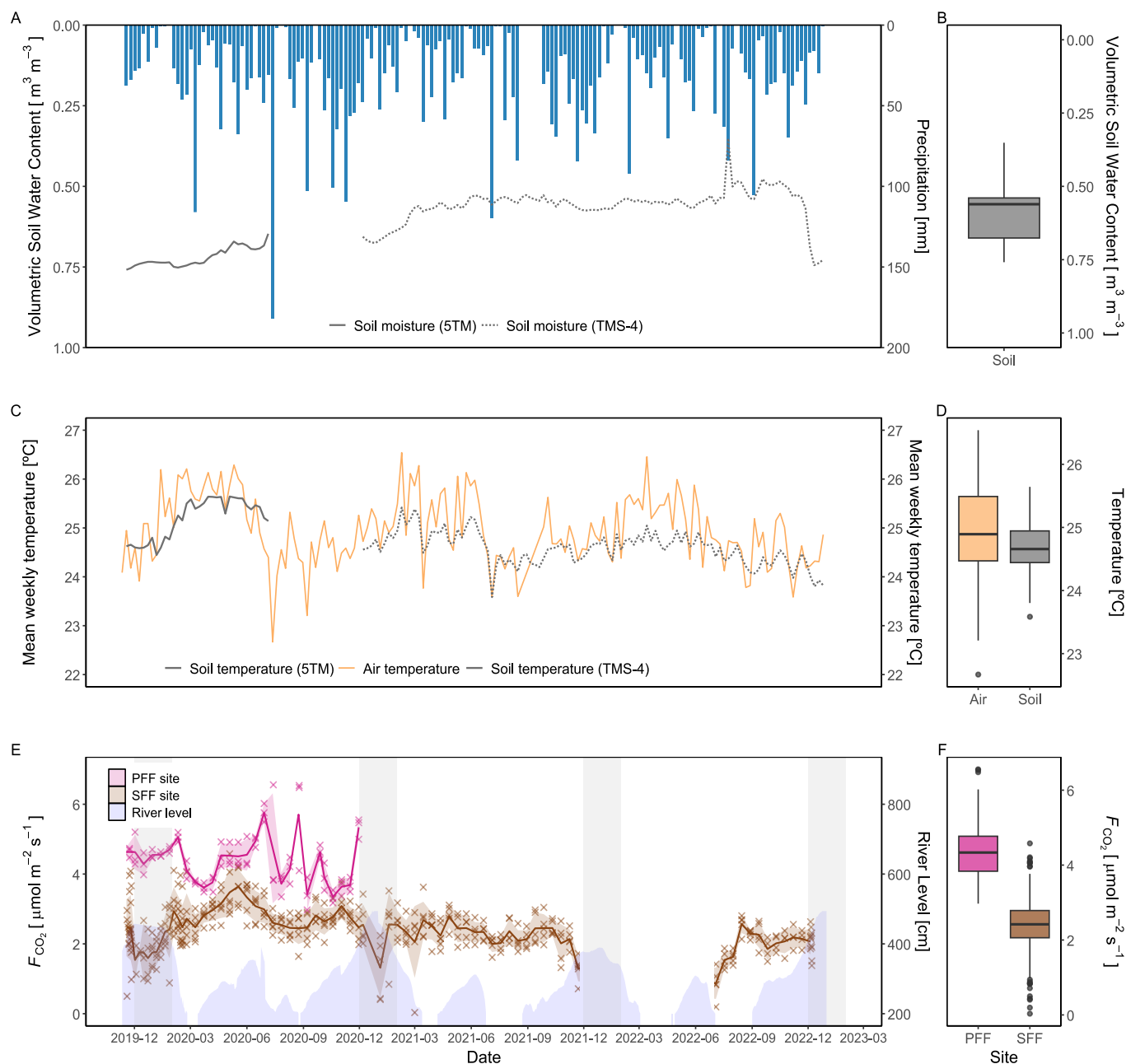


Figure 3. Weekly precipitation, volumetric soil water content, temperature, and CO_2 fluxes. (A) The sum of the weekly precipitation [mm] (blue) obtained from the Trans-African Hydro-Meteorological Monitoring Observatory and mean volumetric soil water content [$\text{m}^3 \text{m}^{-3}$] measured with soil moisture sensors (ECH2O 5TM = solid line, TMS-4 dataloggers = dotted line). (B) Distribution of volumetric soil water content [$\text{m}^3 \text{m}^{-3}$], both sensor types combined. (C) Mean weekly air temperature [$^{\circ}\text{C}$] (gold) was obtained from the Trans-African Hydro-Meteorological Monitoring Observatory. The mean weekly soil temperature [$^{\circ}\text{C}$] was measured with soil temperature sensors (ECH2O 5TM = grey solid line, TMS-4 dataloggers = grey dotted line). (D) Distribution of air and soil temperatures [$^{\circ}\text{C}$], both sensor types combined. (E) Measured surface CO_2 fluxes (cross) [$\mu\text{mol m}^{-2} \text{s}^{-1}$] from the SSF site (brown)

280 and calculated CO₂ fluxes from the PFF site with a K of 3.5 cm h⁻¹(pink). Calculated weekly means (line) and the standard error of the mean are displayed. Blue shading represents river levels (see Section 2.6), while grey bands indicate flooding periods (Dec-Jan) at the SFF site. The displayed time series are discontinuous due to fieldwork constraints (see Section 2.2.) (F) Distribution of surface CO₂ fluxes at the PFF and SFF sites.

3.2.1. Controls on surface CO₂ fluxes at the SSF site

285 The linear mixed effects model (n = 324) explained 43.0 % of the total variability, of which 35.4 % is allocated to the fixed effects (river level, soil moisture and soil temperature; Table 1). The soil temperature and soil moisture are positively correlated with surface CO₂ fluxes. The river level, used as a proxy for the water level, exhibited a quadratic relationship with the CO₂ fluxes measured at the SFF site (Table 1; Figure 4C). The nonlinear component exhibited a negative sign, describing an inverse U-shaped curve (Figure 4C). Initially, the relationship had a positive slope at lower river levels, reaching a maximum point before transitioning to a negative slope. As the river level is used as a proxy for the on-site water level, a short-term campaign 290 was done during the wet season 2023-2024 to confirm the influence of the water level with direct measurements (Unpublished; Supp. Fig. 7). Finally, the significant positive interaction term between temperature and river level suggests a synergistic effect where the combined influence of these two variables on surface fluxes is greater than the addition of their respective individual effects (Figure 4D).

295 **Table 1. Fixed effect estimates for surface CO₂ fluxes at SFF site including river level, soil temperature, and soil moisture as standardized predictors, allowing comparison of their relative importance. For each effect, standard error and p-values (Satterthwaite’s method) are estimated, as well as the marginal (m) and conditional (c) R²_{adj} (Nakagawa et al., 2017).**

Response	Effect	Estimate	SE	P-value	R ² _{adj, m} / R ² _{adj, c}
Surface CO ₂ flux	Intercept	2.61	0.09	< 0.001	0.354/0.430
	River level [1 st degree]	-0.01	0.04	0.833	
	River level [2 nd degree]	-0.19	0.04	< 0.001	
	Soil temperature	0.18	0.04	< 0.001	
	Soil moisture	0.28	0.05	< 0.001	
	River level: Soil Temperature ¹	0.18	0.04	< 0.001	

¹ Interaction term between soil temperature and river level

300 For a deeper understanding of the LMER outputs (Table 1), the individual relationships between surface CO₂ fluxes and the different predictors (soil temperature, river level, and soil moisture) as well as the effect of the interaction between the soil temperature and river level are visualized in Figure 4. The inclusive r² (IR²) of each predictor is also presented, offering a measure of the proportion of variance explained by each predictor, including both its direct effects and interactions with other

predictors (Stoffel et al., 2021). In this context, the soil temperature ($IR^2 = 0.225$), soil moisture ($IR^2 = 0.126$), and the quadratic component of the river level ($IR^2 = 0.097$) appear as the primary factors explaining the variance of surface CO_2 fluxes, whereas the interaction between soil temperature and river level ($IR^2 < 0.001$), along with the linear component of the river level ($IR^2 = 0.001$), make no meaningful contribution (Figure 4)

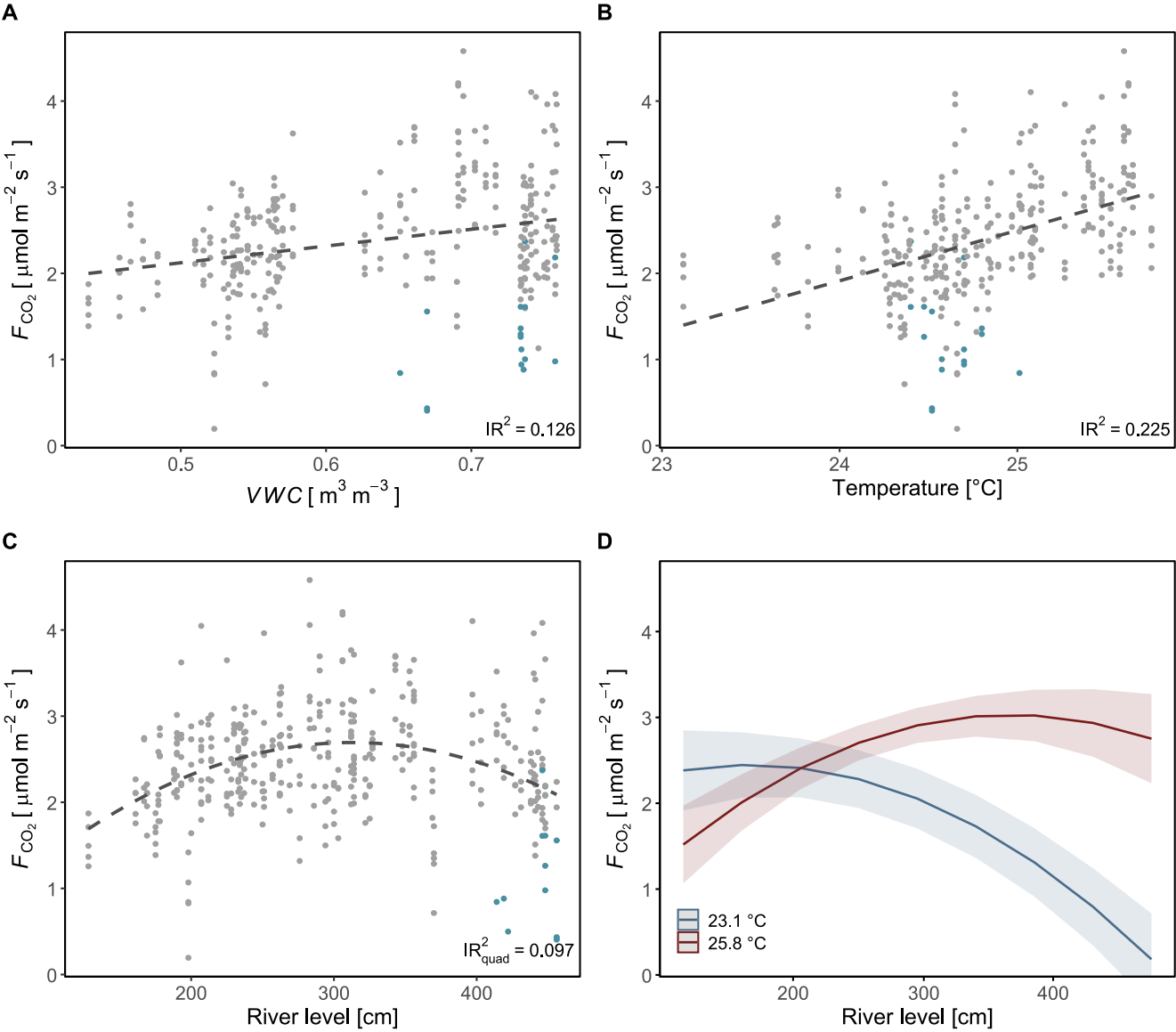


Figure 4. Individual relationships between soil CO_2 fluxes and the environmental parameters (soil moisture (VWC) (A), soil temperature (B), and river level (C)). Measures taken while the soil chamber was partially flooded are represented in blue. Regression lines are displayed as dashed black lines. The interaction between soil temperature and river level is illustrated. Values were predicted based on the LMER model (Table 1) (D). Inclusive r^2 (A, B, C) were estimated based on the LMER model (Table 1; Stoffel et al., 2021).

3.2.2. Controls on surface CO₂ fluxes at the PFF site

315 At the PFF site, surface CO₂ fluxes did not exhibit statistically significant relationships with pH, river level, carbon to nitrogen ratio (C:N), dissolved organic carbon, or biodegradable dissolved organic carbon. Trends were observed, such as an increase in CO₂ fluxes with rising river levels and opposing trends with pH, CO₂ fluxes appeared to decrease as pH increased (Supp. Fig. 7). However, these are just visual tendencies and not statistically significant findings.

3.3 $\delta^{13}\text{C}$ of leaves, litter, soils, soil CO₂ flux, and riverine dissolved CO₂

320 The measured $\delta^{13}\text{C}$ values increased from leaves over litter and SOC to soil CO₂ fluxes and became more positive along this cascade of organic matter transformation (p-values < 0.05; Figure 5). $\delta^{13}\text{C}$ of leaves ranged from -37.1 to -28.9‰ with a mean of $-33.8 \pm 2.1\%$. The $\delta^{13}\text{C}$ signature of litter was between -32.6 and -28.7‰ and, on average $-30.5 \pm 1.0\%$. SOC had $\delta^{13}\text{C}$ of -30.1 to -22.3‰, while the mean was $-27.4 \pm 1.9\%$. The $\delta^{13}\text{C}$ of soil-derived CO₂ (F_{CO2}) was in the range of SOC values for the SFF site (Figure 5) and very stable throughout the measurement period (Supp. Fig. 4). Here, measured $\delta^{13}\text{C}$ values were -
325 30.2 to -26.5‰ with a mean of $-28.5 \pm 0.8\%$. Contrary, the carbon isotopic composition of CO₂ fluxes from the SFF site during flooding was strongly ¹³C enriched with -24.8 to -13.3‰ and an average of $-20.4 \pm 3.4\%$ (p-values < 0.01). The $\delta^{13}\text{C}$ of the inundated soil CO₂ fluxes was higher throughout the whole measurement period (Supp. Fig. 4). The $\delta^{13}\text{C}$ value of dissolved CO₂ from the adjacent Ruki river was highly stable throughout the measurement period from 2022-10 to 2023-06 ranging from -24.9 to -23.3‰ with a mean of $-24.3 \pm 0.5\%$ (Supp. Fig. 4).

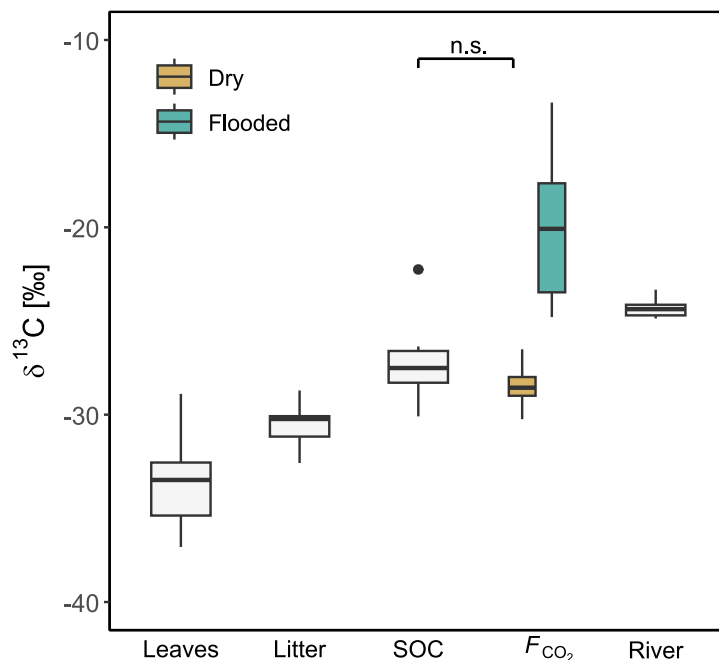


Figure 5. $\delta^{13}\text{C}$ values of leaves, litter, soil organic carbon (SOC), soil CO_2 flux (F) at the SFF site as well as riverine dissolved CO_2 (Ruki river). Surface CO_2 flux (F) is further separated into dry and inundated based on chamber type (floating, static). Non-significant difference between SOC and dry F_{CO_2} is indicated by n.s.

4 Discussion

4.1 CO_2 fluxes

The surface CO_2 flux dataset from the SFF site, measured for three consecutive years, showed intra-seasonal and interannual variability. However, no clear seasonal patterns were observed (Figure 3E). Baumgartner et al. (2020) showed a similar low seasonality in lowland forests of the Congo Basin, attributing it to the limited rainfall variation between dry and wet seasons. The unclear seasonal pattern of the CO_2 fluxes at the SFF site could be attributed to a lasting effect of the flooding on soil moisture (Docherty and Thomas, 2021) and/or consistent rain events during the whole year (Figure 3A-B). These factors, along with the brief duration of both dry seasons, may lead to soil moisture contents remaining near optimal conditions for vegetation and soil microbes to thrive. Such uniform environmental conditions may maintain autotrophic and heterotrophic respiration at a steady level despite undergoing a discernible dry and wet season cycle. The reported mean flux of $2.36 \pm 0.51 \mu\text{mol m}^{-2} \text{s}^{-1}$ from the SFF site was lower compared to previous studies in the Congo Basin. These studies found mean values of respectively $3.13 \pm 1.22 \mu\text{mol m}^{-2} \text{s}^{-1}$, $3.45 \pm 1.14 \mu\text{mol m}^{-2} \text{s}^{-1}$ in montane and lowland forests (Baumgartner et al. 2020) and $4.07 \pm 0.90 \mu\text{mol m}^{-2} \text{s}^{-1}$ in a lowland secondary forest of Cameroon bordering the Congo Basin (Verchot et al., 2020).

Compared to similar tropical forest studies, our values are at the low end of the range reported across the pantropical forest realm (Table 2).

350 The perennially flooded forest site (PFF), located at the interface between terrestrial (forest) and aquatic (stream) ecosystems showed relatively high emissions ($4.38 \pm 0.64 \mu\text{mol m}^{-2} \text{s}^{-1}$) when compared to other tropical flooded forests (Scofield et al. 2016; Table 2) or those streams draining catchments dominated by seasonally or continually inundated swamp forests (Mann et al., 2014; Alin et al. 2011; Table 2). The elevated CO_2 fluxes at the PFF site resulted in higher fluxes relative to the SFF site. Further research is needed to determine whether a greater water depth-integrated respiration (Amaral et al., 2020), a
355 positive correlation with a larger inundated area (Amaral et al., 2020), prolonged river interactions or other factors explain such difference. In contrast, the SFF site presented reduced CO_2 fluxes during the onset of flooding, speculatively due to the inhibitory effect of excessive soil moisture on soil respiration (Courtois et al., 2018; Nissan et al., 2023). A non-significant positive trend between water level and the aquatic CO_2 fluxes was visually discernible (Supp. Fig. 7) which is in line with a positive relationship between $p\text{CO}_2$ and discharge measured on the adjacent Ruki (Drake et al., 2023). As a constant gas transfer
360 velocity was used in the present study, short-term changes in aquatic CO_2 fluxes reflect the variations in carbon dioxide concentrations ($p\text{CO}_2$) in the water. Moreover, the generally low gas transfer velocity (3.5 cm h^{-1}) reflects further the very high $p\text{CO}_2$ concentrations ($10197 - 17260 \text{ ppm}$) measured at the PFF site. These values are significantly higher than the range ($3069 - 9088 \text{ ppm}$) found by Drake et al., (2023). However, the adjacent Ruki water has a long transit time compared to a swamp and a stronger current which in turn results in higher CO_2 outgassing. Generally, the $p\text{CO}_2$ concentration itself is driven
365 by factors such as terrestrial inputs, gas exchange with the atmosphere, water temperature (gas solubility), water chemistry (pH, alkalinity), and in-stream metabolism (Battin et al., 2023; Hotchkiss et al., 2015; Rocher-Ros et al., 2019).

Finally, the *in-situ* derived gas transfer velocity (k_x) expressed as normalized k_{600} (2.95 cm h^{-1}) was higher than the global normalized estimate (k_{600}) for tropical wetlands (2.4 cm h^{-1} ; Aufdenkampe et al. 2011). The gas transfer velocity itself changes
370 by factors influencing the near-surface water turbulence (wind speed, water current velocity). Generally, assuming a constant gas transfer velocity (k_x), as applied in this study, has its limitations since it likely varies throughout the year with increased values during the dry season when the water is flowing in the stream bed channel (Alin et al., 2011).

Table 2. Reported mean values of surface CO₂ fluxes across various tropical forested environments

Country/Basin	Environment	Temporal coverage	Fco ₂ (μmol m ⁻² s ⁻¹)	Source
DRC / Congo Basin	Seasonally flooded forest	3 years	2.36 ± 0.51	This study
	Perennially flooded forest	1 year	4.38 ± 0.64	
DRC / Congo Basin	Montane and lowland (<i>terra firma</i> ¹) forests	3 years, at varying temporal resolution	3.13 to 3.45	Baumgartner et al. (2020)
DRC / Congo Basin	Lowland (<i>terra firma</i> ¹) forest	16 months, sub-daily resolution	4.04 ± 1.16	Daelman et al. (2024)
ROC / Congo Basin	Streams (< 100 m wide) draining swamp forests	3 punctual campaigns over the hydrological year	3.61 ± 1.46	Mann, Spencer, et al. (2014)
Cameroon	Lowland (<i>terra firma</i> ¹) forest	17 months	4.07 ± 0.90	Verchot et al. (2020)
Kenya	Montane (<i>terra firma</i> ¹) forests	2-3 months, dry season and transition period	1.04 to 1.66	Arias-Navarro et al. (2017); Werner, Kiese, and Butterbach-Bahl (2007)
Panama	Lowland poorly drained forest	3 years	4.26 ± 0.16	Rubio and Detto (2017)
Brazil / Amazonian Basin	Seasonally flooded forest	From 1 to 2 years, at varying temporal resolution	2.2 ² to 5.28	Amaral et al. (2020); Borges Pinto et al. (2018); Zanchi et al. (2011)
Brazil / Rio Negro Basin	Perennially flooded forest	Punctual campaigns (low and high-water periods)	0.52 ± 0.21	Scofield et al. (2016)
Brazil / Amazonian Basin	Streams (< 100m wide) draining Amazonian wetlands	Punctual field campaigns integrating low and high flow periods	5.45 ± 3.39 to 5.49 ± 3.16	Alin et al. (2011); Rasera et al. (2008)
Amazonian Basin	Lowland (<i>terra firma</i> ¹) forest	Variable	2.30 to 5.30	(Davidson, Ishida, and Nepstad (2004); Doff sotta et al. (2004); Sousa Neto et al. (2011); Sotta et al. (2007); Garcia-Montiel et al. (2004); Borges Pinto et al. (2018); Janssens, Têtè Barigah, and Ceulemans (1998); Buchmann et al. (1997); Bréchet et al. (2021); Epron et al. (2013); Courtois et al. (2018);
Thailand	Lowland (<i>terra firma</i> ¹) forest	Punctual measurements over 2.5 years	6.57 ± 3.42 ³	Adachi et al. (2009)

Malaysia	Lowland (<i>terra firma</i> ¹) forest	Punctual measurements over 2 and 4 years	5.32 ± 2.85 to 5.7 ± 1.9	Katayama et al. (2009); Ohashi et al. (2007)
Australia	Seasonally flooded forest	13 months	1.4 ± 1.0 / 2.4 ± 1.4 (dry season / wet season)	Goodrick et al. (2016)

375 ¹ *Terra firma* forests refer here to non-flooding forests
² Measurements done only during the inundated period
³ Mean soil respiration for the wet season

4.2 Temperature, soil moisture and water level controls

While the observed CO₂ fluxes at the SFF site showed no clear seasonal pattern, soil temperature, soil moisture and the river level as proxy of the water level emerged as significant controls. While the positive effect of temperature and soil moisture on soil CO₂ fluxes is well known and used to model soil CO₂ fluxes (Nissan et al., 2023), the effect of water level is less well understood. The observed quadratic relationship with the water level suggests an optimal water level beyond which further increases lead to reduced CO₂ fluxes. This optimal point speculatively corresponds to the shift to water saturated conditions in the organic-rich surface soil transitioning from oxic to anoxic conditions. A negative effect of the water level beyond a critical threshold aligns well with the results of Goodrick et al., (2016). That study found maximal soil CO₂ fluxes associated with a water level between 1.5 and 2 m below ground and minimal fluxes when the water level was within 0.15 m of the surface for a tropical riparian swamp forests in Australia (Goodrick et al., 2016). Similarly, Rubio and Detto (2017) found a quadratic relationship between CO₂ fluxes and soil water content in the Amazonian basin. CO₂ fluxes can be reduced in both high and low soil water content, and fluctuations in water level introduce additional factors beyond its influence on soil saturation. Both heterotrophic and autotrophic soil respiration are reduced under dry conditions due to limited microbial activity and reduced photosynthetic activity through stomatal closure (Baumgartner et al. 2020). In our study, the lowest flux event recorded in July 2022 coincided with a marked decrease in soil moisture. This suggests that, during this event, the reduced soil moisture levels became a limiting factor for supporting soil respiration. Conversely, increased soil moisture generally enhances respiration. This was generally the case during our study period, as evidenced by the positive correlation between soil moisture and surface CO₂ fluxes (p-value < 0.05; Table 1). However, excessively high moisture conditions (due to strong rain events or high water level during flooding) can also hinder substrate decomposition by physically impeding the diffusion of atmospheric oxygen and respired CO₂ through the soil pores, thereby limiting both the production and diffusion of CO₂ (Courtois et al., 2018; Nissan et al., 2023). This could explain the temporary decrease in CO₂ fluxes observed at the onset of the flooding period (Figure 3). Furthermore, fluctuations in the water level can influence soil respiration through physical processes like flushing out soil CO₂ during rising phases, enhanced lateral movement of dissolved CO₂, as well as air ingress and redistribution of organic material during receding phases (Dalmagro et al., 2018; Goodrick et al., 2016). Finally, the positive interaction between

soil temperature and water level (p-value < 0.05; Table 1) suggests that higher temperatures will reinforce the effect of the water level and shift the maximum soil flux towards higher water levels delaying its inhibitive effect (Figure 4).

Nevertheless, it is important to note that both the water level and soil moisture measurements exhibit seasonal patterns but do not capture well the short-term changes of the surface CO₂ fluxes at SFF site. Furthermore, the CO₂ fluxes exhibit unclear seasonal pattern (Supp. Fig. 5B). This suggests that other factors, such as aboveground inputs from vegetation, river sediment deposition, and rain-induced events, may significantly influence surface CO₂ fluxes, both in the short term and at seasonal timescales. Additionally, it is important to stress that using river level as a proxy for water level at the SFF site presents limitations such as neglecting local topography or soil characteristics. Thus, fortnightly variations in soil CO₂ fluxes may not be fully captured by this proxy, as local hydrological dynamics might differ from those of the broader river system. Hence, this method may not fully capture the dynamics of the water level and its influence on surface CO₂ fluxes.

Overall, while soil moisture content and temperature are often considered primary drivers of soil CO₂ fluxes (Courtois et al., 2018; Nissan et al., 2023; Oertel et al., 2016), our findings also indicate that incorporating water level can help to unravel the variability of the fluxes for lowland forests with shallow water tables.

At the PFF site, on the other hand, we did not find any statistically significant relationships between potential drivers (DOC, BDOC, river level, pH, C:N) and $p\text{CO}_{2w}$. This suggests that the chemical composition of the water is relatively homogenous throughout the year and that allochthonous rather than autochthonous processes determine $p\text{CO}_{2w}$ concentrations.

4.3 Isotopic indicators

The general carbon isotopic composition of plant tissue is determined by the degree of ¹³C discrimination at the leaf level (Brüggemann et al., 2011). Due to the high photosynthetic activity of tropical plants, ¹³C discrimination is also high, resulting in very negative $\delta^{13}\text{C}$ values at the leaf level as observed in this study (-37.06 to -28.89‰). As the C moves across the various ecosystems C pools, the substrate becomes gradually enriched in ¹³C due to kinetic isotope fractionation. In the case of the studied SFF site, a total ¹³C enrichment of 5.27‰ was observed when moving down the cascade from leaves, litter to SOC and respired CO₂ under dry conditions (p-values < 0.05; Figure 5). Particularly interesting here is the absence of ¹³C fractionation between SOC and soil respired CO₂, which might initially be interpreted as a result of closed system dynamics where the substrate is limited, and organic decomposition tends to be complete. However, soil respired CO₂ is a two-component flux, comprised of heterotrophic and autotrophic respiration. In other words, SOC is not the sole factor governing soil respired CO₂. Indeed, autotrophic respiration is to a large degree fuelled by recently photosynthesized ¹³C depleted carbon (Högberg et al., 2001, Barthel et al., 2011) which in turn can decrease the overall soil respired $\delta^{13}\text{C}$ value relative to SOC (depending on the relative contribution of autotrophic vs heterotrophic soil respiration). Transport rates from above to belowground can reach up to 0.5 m h⁻¹ (Kuzuyakov and Gavrichkova, 2010). Thus, whether the similar $\delta^{13}\text{C}$ values between SOC and respired CO₂ are driven by substrate limitation or a strong influence of autotrophic respiration requires further investigation.

435 The highest ^{13}C enrichment observed was from CO_2 emitted during flooding at the SFF site (-20.4‰; p-values < 0.05). These $\delta^{13}\text{C}$ values were even higher than the $\delta^{13}\text{C}$ values measured in the adjacent Ruki river (-24.30 ‰; p-value < 0.05). The reason for such highly ^{13}C enriched CO_2 outgassing during inundation remains unclear but given that the water in the inundated forest likely experiences relatively long residence times compared to the river, the outgassed CO_2 might become this heavily ^{13}C -enriched due to extensive outgassing. Moreover, the standing water allows the growth of methanogenic archaea which use
440 simple carbon compounds such as acetate as electron donors (Conrad et al., 2021). The CO_2 molecules obtained from acetate cleavage is another fractionation process which potentially influences the overall isotopic composition of outgassed CO_2 . Lastly, as the inundation of the SFF site is mainly driven by backflow from the river system, the dissolved CO_2 in the inundated water could be a mix of riverine and locally soil-respired CO_2 that undergoes further *in-situ* ^{13}C enrichment.

5 Conclusion

445 This study presents a multi-year dataset of CO_2 fluxes from two forested wetland sites along a flooding gradient : a seasonally flooded forest (SFF) and a perennially flooded forest (PFF). While exhibiting short-term and interannual fluctuations, CO_2 fluxes showed limited seasonal patterns. At the SFF site, surface emissions increased with rising soil moisture and temperature, while the water level demonstrated a significant quadratic relationship. Despite the significant sensitivity to environmental conditions over the observation period, the short-term variability observed at both sites, as well as the interannual variability
450 at the SFF site, were incompletely explained, suggesting the influence of additional factors in regulating emissions.

Our results emphasize that water level, alongside soil temperature and soil moisture, significantly affects surface CO_2 fluxes in lowland areas with shallow, fluctuating water tables. Future research should include direct measurements of the water level over the entire hydrological year to elucidate the temporal dynamics of this relationship. Overall, the reported measurements
455 contribute to filling the data gap for soil respiration rates of tropical forests in the Congo Basin and provide baseline fluxes for parametrizing earth system models.

Data Availability

The datasets generated in this study have been deposited in the Zenodo repository (<https://doi.org/10.5281/zenodo.15051088>) and are available from the corresponding author upon request. Additionally, the data used in this study has been made available
460 through the soil respiration database (SRDB; Jian, J. et al. 2021).

Author contributions

Mbarthel, MBauters, TWD, KVO, and JS were responsible for study design and conceived the study. Fieldwork was conducted by Mbarthel, MBauters, TWD, SB, NBM, JC, ADC, and CE. Lab work was conducted by Mbarthel, RAW, SB and JC. Data analyzes and interpretation was performed by ACHJ, ADC, MBauters and Mbarthel. ADC and ACHJ wrote the manuscript with contributions from all co-authors.

Competing Interests

At least one of the (co-)authors is a member of the editorial board of Biogeosciences.

Acknowledgements

The authors would like to thank the Trans-African Hydro-Meteorological Monitoring Observatory (TAHMO) for providing meteorological data from the investigated site and the ICCN park guards for assistance in the field. The authors would like to further thank Annika Ackermann from the Grassland Science group (Prof. Buchmann) at ETH Zurich for the stable isotope analysis of plant and soil materials.

Funding Statement

The core funding of ETH Zurich financed this study. MBarthel received funding from the Swiss National Science Foundation (IZSEZ0_186376 / 1).

References

- Adachi, M., Ishida, A., Bunyavejchewin, S., Okuda, T., and Koizumi, H.: Spatial and temporal variation in soil respiration in a seasonally dry tropical forest, Thailand, *J. Trop. Ecol.*, 25, 531–539, <https://doi.org/10.1017/S026646740999006X>, 2009.
- Alin, S. R., de Fátima F. L. Rasera, M., Salimon, C. I., Richey, J. E., Holtgrieve, G. W., Krusche, A. V., and Snidvongs, A.: Physical controls on carbon dioxide transfer velocity and flux in low-gradient river systems and implications for regional carbon budgets, *J. Geophys. Res. Biogeosciences*, 116, <https://doi.org/10.1029/2010JG001398>, 2011.
- Alsdorf, D., Beighley, E., Laraque, A., Lee, H., Tshimanga, R., O’Loughlin, F., Mahé, G., Dinga, B., Moukandi, G., and Spencer, R. G. M.: Opportunities for hydrologic research in the Congo Basin, *Rev. Geophys.*, 54, 378–409, <https://doi.org/10.1002/2016RG000517>, 2016.
- Amaral, J. H. F., Melack, J. M., Barbosa, P. M., MacIntyre, S., Kasper, D., Cortés, A., Silva, T. S. F., Nunes de Sousa, R., and Forsberg, B. R.: Carbon Dioxide Fluxes to the Atmosphere From Waters Within Flooded Forests in the Amazon Basin, *J. Geophys. Res. Biogeosciences*, 125, e2019JG005293, <https://doi.org/10.1029/2019JG005293>, 2020.

- Arias-Navarro, C., Díaz-Pinés, E., Klatt, S., Brandt, P., Rufino, M. C., Butterbach-Bahl, K., and Verchot, L. V.: Spatial variability of soil N₂O and CO₂ fluxes in different topographic positions in a tropical montane forest in Kenya, *J. Geophys. Res. Biogeosciences*, 122, 514–527, <https://doi.org/10.1002/2016JG003667>, 2017.
- Aufdenkampe, A. K., Mayorga, E., Raymond, P. A., Melack, J. M., Doney, S. C., Alin, S. R., Aalto, R. E., and Yoo, K.: Riverine coupling of biogeochemical cycles between land, oceans, and atmosphere, *Front. Ecol. Environ.*, 9, 53–60, <https://doi.org/10.1890/100014>, 2011.
- Barthel, M., Bauters, M., Baumgartner, S., Drake, T. W., Bey, N. M., Bush, G., Boeckx, P., Botefa, C. I., Dériaz, N., Ekamba, G. L., Gallarotti, N., Mbayu, F. M., Mugula, J. K., Makelele, I. A., Mbongo, C. E., Mohn, J., Mande, J. Z., Mpambi, D. M., Ntaboba, L. C., Rukeza, M. B., Spencer, R. G. M., Summerauer, L., Vanlauwe, B., Van Oost, K., Wolf, B., and Six, J.: Low N₂O and variable CH₄ fluxes from tropical forest soils of the Congo Basin, *Nat. Commun.*, 13, 330, <https://doi.org/10.1038/s41467-022-27978-6>, 2022.
- Barton, K.: MuMIn: multi-model inference. R package version 1.43. 17, 2020.
- Bastviken, D., Tranvik, L. J., Downing, J. A., Crill, P. M., and Enrich-Prast, A.: Freshwater Methane Emissions Offset the Continental Carbon Sink, *Science*, 331, 50–50, <https://doi.org/10.1126/science.1196808>, 2011.
- Bates, D., Mächler, M., Bolker, B., and Walker, S.: Fitting Linear Mixed-Effects Models Using lme4, *J. Stat. Softw.*, 67, 1–48, <https://doi.org/10.18637/jss.v067.i01>, 2015.
- Battin, T. J., Lauerwald, R., Bernhardt, E. S., Bertuzzo, E., Gener, L. G., Hall, R. O., Hotchkiss, E. R., Maavara, T., Pavelsky, T. M., Ran, L., Raymond, P., Rosentreter, J. A., and Regnier, P.: River ecosystem metabolism and carbon biogeochemistry in a changing world, *Nature*, 613, 449–459, <https://doi.org/10.1038/s41586-022-05500-8>, 2023.
- Baumgartner, S., Barthel, M., Drake, T. W., Bauters, M., Makelele, I. A., Mugula, J. K., Summerauer, L., Gallarotti, N., Cizungu Ntaboba, L., Van Oost, K., Boeckx, P., Doetterl, S., Werner, R. A., and Six, J.: Seasonality, drivers, and isotopic composition of soil CO₂ fluxes from tropical forests of the Congo Basin, *Biogeosciences*, 17, 6207–6218, <https://doi.org/10.5194/bg-17-6207-2020>, 2020a.
- Baumgartner, S., Barthel, M., Drake, T. W., Bauters, M., Makelele, I. A., Mugula, J. K., Summerauer, L., Gallarotti, N., Ntaboba, L. C., Van Oost, K., Boeckx, P., Doetterl, S., Werner, R. A., and Six, J.: Seasonality, drivers, and isotopic composition of soil CO₂ fluxes from tropical forests of the Congo Basin, *Biogeochemistry: Greenhouse Gases*, <https://doi.org/10.5194/bg-2020-133>, 2020b.
- Borges, A. V., Abril, G., Darchambeau, F., Teodoru, C. R., Deborde, J., Vidal, L. O., Lambert, T., and Bouillon, S.: Divergent biophysical controls of aquatic CO₂ and CH₄ in the World's two largest rivers, *Sci. Rep.*, 5, 1–10, <https://doi.org/10.1038/srep15614>, 2015a.
- Borges, A. V., Darchambeau, F., Teodoru, C. R., Marwick, T. R., Tamooch, F., Geeraert, N., Omengo, F. O., Guérin, F., Lambert, T., Morana, C., Okuku, E., and Bouillon, S.: Globally significant greenhouse-gas emissions from African inland waters, *Nat. Geosci.*, 8, 637–642, <https://doi.org/10.1038/ngeo2486>, 2015b.
- Borges, A. V., Darchambeau, F., Lambert, T., Morana, C., Allen, G. H., Tambwe, E., Toengaho Sembaito, A., Mambo, T., Wabakhangazi, J. N., Descy, J. P., Teodoru, C. R., and Bouillon, S.: Variations in dissolved greenhouse gases (CO₂, CH₄, N₂O) in the Congo River network overwhelmingly driven by fluvial-wetland connectivity, *Biogeosciences*, 16, 3801–3834, <https://doi.org/10.5194/bg-16-3801-2019>, 2019.

- 525 Borges Pinto, O., Vourlitis, G. L., De Souza Carneiro, E. M., De França Dias, M., Hentz, C., and De Souza Nogueira, J.: Interactions between Vegetation, Hydrology, and Litter Inputs on Decomposition and Soil CO₂ Efflux of Tropical Forests in the Brazilian Pantanal, *Forests*, 9, 281, <https://doi.org/10.3390/f9050281>, 2018.
- Bouillon, S., Yambélé, A., Spencer, R. G. M., Gillikin, D. P., Hernes, P. J., Six, J., Merckx, R., and Borges, A. V.: Organic matter sources, fluxes and greenhouse gas exchange in the Oubangui River (Congo River basin), *Biogeosciences*, 9, 2045–2062, <https://doi.org/10.5194/bg-9-2045-2012>, 2012.
- Bréchet, L. M., Daniel, W., Stahl, C., Burban, B., Goret, J.-Y., Salomón, R. L., and Janssens, I. A.: Simultaneous tree stem and soil greenhouse gas (CO₂, CH₄, N₂O) flux measurements: a novel design for continuous monitoring towards improving flux estimates and temporal resolution, *New Phytol.*, 230, 2487–2500, <https://doi.org/10.1111/nph.17352>, 2021.
- 535 Breitengroß, J. P.: Saisonales Fließverhalten in großflächigen Flußsystemen. Methoden zur Erfassung und Darstellung am Beispiel des Kongo (Zaire), *Mitteilungen Geogr. Ges. Hambg.*, 60, 1–92, 1972.
- Brooks, P. D., Geilmann, H., Werner, R. A., and Brand, W. A.: Improved precision of coupled $\delta^{13}\text{C}$ and $\delta^{15}\text{N}$ measurements from single samples using an elemental analyzer/isotope ratio mass spectrometer combination with a post-column six-port valve and selective CO₂ trapping; improved halide robustness of the combustion reactor using CeO₂, *Rapid Commun. Mass Spectrom.*, 17, 1924–1926, <https://doi.org/10.1002/rcm.1134>, 2003.
- 540 Buchmann, N., Guehl, J.-M., Barigah, T. S., and Ehleringer, J. R.: Interseasonal comparison of CO₂ concentrations, isotopic composition, and carbon dynamics in an Amazonian rainforest (French Guiana), *Oecologia*, 110, 120–131, <https://doi.org/10.1007/s004420050140>, 1997.
- Conrad, R., Liu, P., and Claus, P.: Fractionation of stable carbon isotopes during acetate consumption by methanogenic and sulfidogenic microbial communities in rice paddy soils and lake sediments, *Biogeosciences*, 18, 6533–6546, <https://doi.org/10.5194/bg-18-6533-2021>, 2021.
- 545 Courtois, E. A., Stahl, C., Van den Berge, J., Bréchet, L., Van Langenhove, L., Richter, A., Urbina, I., Soong, J. L., Peñuelas, J., and Janssens, I. A.: Spatial Variation of Soil CO₂, CH₄ and N₂O Fluxes Across Topographical Positions in Tropical Forests of the Guiana Shield, *Ecosystems*, 21, 1445–1458, <https://doi.org/10.1007/s10021-018-0232-6>, 2018.
- 550 Crezee, B., Dargie, G. C., Ewango, C. E. N., Mitchard, E. T. A., Emba B., O., Kanyama T., J., Bola, P., Ndjango, J.-B. N., Girkin, N. T., Bocko, Y. E., Ifo, S. A., Hubau, W., Seidensticker, D., Batumike, R., Imani, G., Cuní-Sanchez, A., Kiahtipes, C. A., Lebamba, J., Wotzka, H.-P., Bean, H., Baker, T. R., Baird, A. J., Boom, A., Morris, P. J., Page, S. E., Lawson, I. T., and Lewis, S. L.: Mapping peat thickness and carbon stocks of the central Congo Basin using field data, *Nat. Geosci.*, 15, 639–644, <https://doi.org/10.1038/s41561-022-00966-7>, 2022.
- 555 Daelman, R., Bauters, M., Barthel, M., Bulonza, E., Lefevre, L., Mbifo, J., Six, J., Butterbach-Bahl, K., Wolf, B., Kiese, R., and Boeckx, P.: Spatiotemporal variability of CO₂, N₂O and CH₄ fluxes from a semi-deciduous tropical forest soil in the Congo basin, *EGU sphere*, 1–21, <https://doi.org/10.5194/egusphere-2024-2346>, 2024.
- Dalmagro, H. J., Lathuillière, M. J., Hawthorne, I., Morais, D. D., Pinto Jr, O. B., Couto, E. G., and Johnson, M. S.: Carbon biogeochemistry of a flooded Pantanal forest over three annual flood cycles, *Biogeochemistry*, 139, 1–18, <https://doi.org/10.1007/s10533-018-0450-1>, 2018.
- 560 Davidson, E. A., Ishida, F. Y., and Nepstad, D. C.: Effects of an experimental drought on soil emissions of carbon dioxide, methane, nitrous oxide, and nitric oxide in a moist tropical forest, *Glob. Change Biol.*, 10, 718–730, <https://doi.org/10.1111/j.1365-2486.2004.00762.x>, 2004.

- Docherty, E. M. and Thomas, A. D.: Larger floods reduce soil CO₂ efflux during the post-flooding phase in seasonally-flooded forests of Western Amazonia, *Pedosphere*, 31, 342–352, [https://doi.org/10.1016/S1002-0160\(20\)60073-X](https://doi.org/10.1016/S1002-0160(20)60073-X), 2021.
- 565 Doff sotta, E., Meir, P., Malhi, Y., Donato nobre, A., Hodnett, M., and Grace, J.: Soil CO₂ efflux in a tropical forest in the central Amazon, *Glob. Change Biol.*, 10, 601–617, <https://doi.org/10.1111/j.1529-8817.2003.00761.x>, 2004.
- Drake, T. W., Raymond, P. A., and Spencer, R. G. M.: Terrestrial carbon inputs to inland waters: A current synthesis of estimates and uncertainty, *Limnol. Oceanogr. Lett.*, 3, 132–142, <https://doi.org/10.1002/lol2.10055>, 2018.
- 570 Drake, T. W., Barthel, M., Mbongo, C. E., Mpambi, D. M., Baumgartner, S., Botefa, C. I., Bauters, M., Kurek, M. R., Spencer, R. G. M., McKenna, A. M., Haghipour, N., Ekamba, G. L., Wabakanghanzi, J. N., Eglinton, T. I., Van Oost, K., and Six, J.: Hydrology drives export and composition of carbon in a pristine tropical river, *Limnol. Oceanogr.*, 68, 2476–2491, <https://doi.org/10.1002/lno.12436>, 2023.
- 575 Epron, D., Nouvellon, Y., Mareschal, L., Moreira, R. M. e, Koutika, L.-S., Geneste, B., Delgado-Rojas, J. S., Laclau, J.-P., Sola, G., Gonçalves, J. L. de M., and Bouillet, J.-P.: Partitioning of net primary production in Eucalyptus and Acacia stands and in mixed-species plantations: Two case-studies in contrasting tropical environments, *For. Ecol. Manag.*, 301, 102–111, <https://doi.org/10.1016/j.foreco.2012.10.034>, 2013.
- Gallarotti, N., Barthel, M., Verhoeven, E., Pereira, E. I. P., Bauters, M., Baumgartner, S., Drake, T. W., Boeckx, P., Mohn, J., Longepierre, M., Mugula, J. K., Makelele, I. A., Ntaboba, L. C., and Six, J.: In-depth analysis of N₂O fluxes in tropical forest soils of the Congo Basin combining isotope and functional gene analysis, *ISME J.*, 15, 3357–3374, <https://doi.org/10.1038/s41396-021-01004-x>, 2021.
- 580 Garcia-Montiel, D. C., Melillo, J. M., Steudler, P. A., Tian, H., Neill, C., Kicklighter, D. W., Feigl, B., Piccolo, M., and Cerri, C. C.: Emissions of N₂o and Co₂ from Terra Firme Forests in Rondônia, Brazil, *Ecol. Appl.*, 14, 214–220, <https://doi.org/10.1890/01-6023>, 2004.
- Georgiou, S., Mitchard, E. T. A., Crezee, B., Dargie, G. C., Young, D. M., Jovani-Sancho, A. J., Kitambo, B., Papa, F., Bocko, Y. E., Bola, P., Crabtree, D. E., Emba, O. B., Ewango, C. E. N., Girkin, N. T., Ifo, S. A., Kanyama, J. T., Mampouya, Y. E. W., Mbemba, M., Ndjango, J.-B. N., Palmer, P. I., Sjögersten, S., and Lewis, S. L.: Mapping Water Levels across a Region of the Cuvette Centrale Peatland Complex, *Remote Sens.*, 15, 3099, <https://doi.org/10.3390/rs15123099>, 2023.
- Goodrick, I., Connor, S., Bird, M. I., and Nelson, P. N.: Emission of CO₂ from tropical riparian forest soil is controlled by soil temperature, soil water content and depth to water table, *Soil Res.*, 54, 311, <https://doi.org/10.1071/SR15040>, 2016.
- 590 Grolemond, G. and Wickham, H.: Dates and times made easy with lubridate, *J. Stat. Softw.*, 40, 1–25, <https://doi.org/10.18637/jss.v040.i03>, 2011.
- Hashimoto, S., Carvalhais, N., Ito, A., Migliavacca, M., Nishina, K., and Reichstein, M.: Global spatiotemporal distribution of soil respiration modeled using a global database, 2015.
- 595 Hotchkiss, E. R., Hall Jr, R. O., Sponseller, R. A., Butman, D., Klaminder, J., Laudon, H., Rosvall, M., and Karlsson, J.: Sources of and processes controlling CO₂ emissions change with the size of streams and rivers, *Nat. Geosci.*, 8, 696–699, <https://doi.org/10.1038/ngeo2507>, 2015.
- Huang, N., Wang, L., Song, X.-P., Black, T. A., and Niu, Z.: Spatial and temporal variations in global soil respiration and their relationships with climate and land cover, *Science Advances*, <https://doi.org/10.1126/sciadv.abb8508>, 2020.

- Hubau, W., Lewis, S. L., Phillips, O. L., Affum-Baffoe, K., Beeckman, H., Cuní-Sánchez, A., Daniels, A. K., Ewango, C. E. N., Fauset, S., Mukinzi, J. M., Sheil, D., Sonké, B., Sullivan, M. J. P., Sunderland, T. C. H., Taedoumg, H., Thomas, S. C., White, L. J. T., Abernethy, K. A., Adu-Bredu, S., Amani, C. A., Baker, T. R., Banin, L. F., Baya, F., Begne, S. K., Bennett, A. C., Benedet, F., Bitariho, R., Bocko, Y. E., Boeckx, P., Boundja, P., Brienens, R. J. W., Brncic, T., Chezeaux, E., Chuyong, G. B., Clark, C. J., Collins, M., Comiskey, J. A., Coomes, D. A., Dargie, G. C., de Haulleville, T., Kamdem, M. N. D., Doucet, J. L., Esquivel-Muelbert, A., Feldpausch, T. R., Fofanah, A., Foli, E. G., Gilpin, M., Gloor, E., Gonmadje, C., Gourlet-Fleury, S., Hall, J. S., Hamilton, A. C., Harris, D. J., Hart, T. B., Hockemba, M. B. N., Hladik, A., Ifo, S. A., Jeffery, K. J., Jucker, T., Yakusu, E. K., Kearsley, E., Kenfack, D., Koch, A., Leal, M. E., Levesley, A., Lindsell, J. A., Lisingo, J., Lopez-Gonzalez, G., Lovett, J. C., Makana, J. R., Malhi, Y., Marshall, A. R., Martin, J., Martin, E. H., Mbayu, F. M., Medjibe, V. P., Mihindou, V., Mitchard, E. T. A., Moore, S., Munishi, P. K. T., Bengone, N. N., Ojo, L., Ondo, F. E., Peh, K. S. H., Pickavance, G. C., Poulsen, A. D., Poulsen, J. R., Qie, L., Reitsma, J., Rovero, F., Swaine, M. D., Talbot, J., Taplin, J., Taylor, D. M., Thomas, D. W., Toirambe, B., Mukendi, J. T., Tuagben, D., Umunay, P. M., et al.: Asynchronous carbon sink saturation in African and Amazonian tropical forests, *Nature*, 579, 80–87, <https://doi.org/10.1038/s41586-020-2035-0>, 2020.
- Janssens, I. A., Tête Barigah, S., and Ceulemans, R.: Soil CO₂ efflux rates in different tropical vegetation types in French Guiana, *Ann. Sci. For.*, 55, 671–680, <https://doi.org/10.1051/forest:19980603>, 1998.
- Jian, J., Vargas, R., Anderson-Teixeira, K.J., Stell, E., Herrmann, V., Horn, M., Kholod, N., Manzon, J., Marchesi, R., Paredes, D., and Bond-Lamberty, B.P.: Soil CollectionA Global Database of Soil Respiration Data, Version 5.0, 0 MB, <https://doi.org/10.3334/ORNDAAC/1827>, 2021.
- Katayama, A., Kume, T., Komatsu, H., Ohashi, M., Nakagawa, M., Yamashita, M., Otsuki, K., Suzuki, M., and Kumagai, T.: Effect of forest structure on the spatial variation in soil respiration in a Bornean tropical rainforest, *Agric. For. Meteorol.*, 149, 1666–1673, <https://doi.org/10.1016/j.agrformet.2009.05.007>, 2009.
- Keeling, D.: The concentration and isotopic abundances of atmospheric carbon dioxide in rural areas, *Geochim. Cosmochim. Acta*, 13, 322–334, 1958.
- Kuznetsova, A., Brockhoff, P. B., and Christensen, R. H. B.: lmerTest Package: Tests in Linear Mixed Effects Models, *J. Stat. Softw.*, 82, <https://doi.org/10.18637/jss.v082.i13>, 2017.
- Kuzyakov, Y. and Gavrichkova, O.: REVIEW: Time lag between photosynthesis and carbon dioxide efflux from soil: a review of mechanisms and controls, *Glob. Change Biol.*, 16, 3386–3406, <https://doi.org/10.1111/j.1365-2486.2010.02179.x>, 2010.
- Lewis, S. L., Sonké, B., Sunderland, T., Begne, S. K., Lopez-Gonzalez, G., van der Heijden, G. M. F., Phillips, O. L., Affum-Baffoe, K., Baker, T. R., Banin, L., Bastin, J.-F., Beeckman, H., Boeckx, P., Bogaert, J., De Cannière, C., Chezeaux, E., Clark, C. J., Collins, M., Djabbletey, G., Djuikouo, M. N. K., Droissart, V., Doucet, J.-L., Ewango, C. E. N., Fauset, S., Feldpausch, T. R., Foli, E. G., Gillet, J.-F., Hamilton, A. C., Harris, D. J., Hart, T. B., de Haulleville, T., Hladik, A., Hufkens, K., Huygens, D., Jeanmart, P., Jeffery, K. J., Kearsley, E., Leal, M. E., Lloyd, J., Lovett, J. C., Makana, J.-R., Malhi, Y., Marshall, A. R., Ojo, L., Peh, K. S. H., Pickavance, G., Poulsen, J. R., Reitsma, J. M., Sheil, D., Simo, M., Steppe, K., Taedoumg, H. E., Talbot, J., Taplin, J. R. D., Taylor, D., Thomas, S. C., Toirambe, B., Verbeeck, H., Vleminckx, J., White, L. J. T., Willcock, S., Woell, H., and Zemagho, L.: Above-ground biomass and structure of 260 African tropical forests, *Philos. Trans. R. Soc. B Biol. Sci.*, 368, 20120295, <https://doi.org/10.1098/rstb.2012.0295>, 2013.
- Lüdecke, D.: sjPlot: Data Visualization for Statistics in Social Science, <https://doi.org/10.32614/CRAN.package.sjPlot>, 2013.
- Mann, P. J., Tffail, M. M., Cooper, W. T., Kostka, J. E., Chanton, P. R., Schadt, C. W., Hanson, P. J., Iversen, C. M., Chanton, J. P., and Mann, P. J.: Journal of Geophysical Research: Biogeosciences, *J. Geophys. Res. Biogeosciences*, 661–675, <https://doi.org/10.1002/2013JG002442>.Received, 2014a.

- 640 Mann, P. J., Spencer, R. G. M., Dinga, B. J., Poulsen, J. R., Hernes, P. J., Fiske, G., Salter, M. E., Wang, Z. A., Hoering, K. A., Six, J., and Holmes, R. M.: The biogeochemistry of carbon across a gradient of streams and rivers within the Congo Basin, *J. Geophys. Res. Biogeosciences*, 119, 687–702, <https://doi.org/10.1002/2013JG002442>, 2014b.
- Mann, P. J., Spencer, R. G. M., Dinga, B. J., Poulsen, J. R., Hernes, P. J., Fiske, G., Salter, M. E., Wang, Z. A., Hoering, K. A., Six, J., and Holmes, R. M.: The biogeochemistry of carbon across a gradient of streams and rivers within the Congo Basin, *J. Geophys. Res. Biogeosciences*, 119, 687–702, <https://doi.org/10.1002/2013JG002442>, 2014c.
- 645 Mitchard, E. T. A.: The tropical forest carbon cycle and climate change, *Nature*, 559, 527–534, <https://doi.org/10.1038/s41586-018-0300-2>, 2018.
- Nakagawa, S., Johnson, P. C. D., and Schielzeth, H.: The coefficient of determination R² and intra-class correlation coefficient from generalized linear mixed-effects models revisited and expanded, *J. R. Soc. Interface*, 14, 20170213, <https://doi.org/10.1098/rsif.2017.0213>, 2017.
- 650 Nissan, A., Alcolombri, U., Peleg, N., Galili, N., Jimenez-Martinez, J., Molnar, P., and Holzner, M.: Global warming accelerates soil heterotrophic respiration, *Nat. Commun.*, 14, 3452, <https://doi.org/10.1038/s41467-023-38981-w>, 2023.
- Oertel, C., Matschullat, J., Zurba, K., Zimmermann, F., and Erasmi, S.: Greenhouse gas emissions from soils—A review, *Chem. Erde - Geochem.*, 76, <https://doi.org/10.1016/j.chemer.2016.04.002>, 2016.
- Ohashi, M., Kume, T., Yamane, S., and Suzuki, M.: Hot spots of soil respiration in an Asian tropical rainforest, *Geophys. Res. Lett.*, 34, <https://doi.org/10.1029/2007GL029587>, 2007.
- 655 Parmentier, I., Malhi, Y., Senterre, B., Whittaker, R. J., and ALONSO, A., Balinga, M. P. B., Bakayoko, A., Bongers, F., ChaTELain, C., Comiskey, J. A., Cortay, R., Kamdem, M.-N. D., Doucet, J.-L., Gautier, L., Hawthorne, W. D., Issembe, Y. A., Kouamé, F. N., Kouka, L. A., Leal, M. E., Lejoly, J., Lewis, S. L., Nusbaumer, L., Parren, M. P. E., Peh, K. S.-H., Phillips, O. L., Sheil, D., Sonké, B., Sosef, M. S. M., Sunderland, T. C. H., Stropp, J., Ter Steege, H., Swaine, M. D., Tchouto, M. G. P., Gernerden, B. S. V., Van Valkenburg, J. L. C. H., and Wöll, H.: The odd man out? Might climate explain the lower tree α -diversity of African rain forests relative to Amazonian rain forests?, *J. Ecol.*, 95, 1058–1071, <https://doi.org/10.1111/j.1365-2745.2007.01273.x>, 2007.
- 660 Pavelka, M., Acosta, M., Kiese, R., Altimir, N., Brümmer, C., Crill, P., Darenova, E., Fuß, R., Gielen, B., Graf, A., Klemetsson, L., Lohila, A., Longdoz, B., Lindroth, A., Nilsson, M., Jiménez, S. M., Merbold, L., Montagnani, L., Peichl, M., Pihlatie, M., Pumpanen, J., Ortiz, P. S., Silvennoinen, H., Skiba, U., Vestin, P., Weslien, P., Janous, D., and Kutsch, W.: Standardisation of chamber technique for CO₂, N₂O and CH₄ fluxes measurements from terrestrial ecosystems, *Int. Agrophysics*, 32, 569–587, <https://doi.org/10.1515/intag-2017-0045>, 2018.
- Pelletier, L., Strachan, I. B., Garneau, M., and Roulet, N. T.: Carbon release from boreal peatland open water pools: Implication for the contemporary C exchange, *J. Geophys. Res. Biogeosciences*, 119, 207–222, <https://doi.org/10.1002/2013JG002423>, 2014.
- 670 R Core Team: R: A Language and Environment for Statistical Computing, 2023.
- Rasera, M. de F. F. L., Ballester, M. V. R., Krusche, A. V., Salimon, C., Montebelo, L. A., Alin, S. R., Victoria, R. L., and Richey, J. E.: Estimating the Surface Area of Small Rivers in the Southwestern Amazon and Their Role in CO₂ Outgassing, *Earth Interact.*, 12, 1–16, <https://doi.org/10.1175/2008EI257.1>, 2008.

- 675 Raymond, P. A., Hartmann, J., Lauerwald, R., Sobek, S., McDonald, C., Hoover, M., Butman, D., Striegl, R., Mayorga, E., Humborg, C., Kortelainen, P., Dürr, H., Meybeck, M., Ciais, P., and Guth, P.: Global carbon dioxide emissions from inland waters, *Nature*, 503, 355–359, <https://doi.org/10.1038/nature12760>, 2013.
- Rocher-Ros, G., Sponseller, R. A., Lidberg, W., Mörtz, C.-M., and Giesler, R.: Landscape process domains drive patterns of CO₂ evasion from river networks, *Limnol. Oceanogr. Lett.*, 4, 87–95, <https://doi.org/10.1002/lol2.10108>, 2019.
- 680 Rosentreter, J. A., Borges, A. V., Deemer, B. R., Holgerson, M. A., Liu, S., Song, C., Melack, J., Raymond, P. A., Duarte, C. M., Allen, G. H., Olefeldt, D., Poulter, B., Battin, T. I., and Eyre, B. D.: Half of global methane emissions come from highly variable aquatic ecosystem sources, *Nat. Geosci.*, 14, 225–230, <https://doi.org/10.1038/s41561-021-00715-2>, 2021.
- RStudio Team: RStudio: Integrated Development Environment for R, 2023.
- Rubio, V. E. and Detto, M.: Spatiotemporal variability of soil respiration in a seasonal tropical forest, *Ecol. Evol.*, 7, 7104–7116, <https://doi.org/10.1002/ece3.3267>, 2017.
- 685 Runge, J.: The Congo River, Central Africa, in: *Large Rivers: Geomorphology and Management*, edited by: Gupta, A., John Wiley & Sons, Ltd, West Sussex, 293–308, 2007.
- Scofield, V., Melack, J. M., Barbosa, P. M., Amaral, J. H. F., Forsberg, B. R., and Farjalla, V. F.: Carbon dioxide outgassing from Amazonian aquatic ecosystems in the Negro River basin, *Biogeochemistry*, 129, 77–91, <https://doi.org/10.1007/s10533-016-0220-x>, 2016.
- 690 Slik, J. W. F., Arroyo-Rodríguez, V., Aiba, S.-I., Alvarez-Loayza, P., Alves, L. F., Ashton, P., Balvanera, P., Bastian, M. L., Bellingham, P. J., van den Berg, E., Bernacci, L., da Conceição Bispo, P., Blanc, L., Böhning-Gaese, K., Boeckx, P., Bongers, F., Boyle, B., Bradford, M., Brearley, F. Q., Breuer-Ndoundou Hockemba, M., Bunyavejchewin, S., Calderado Leal Matos, D., Castillo-Santiago, M., Catharino, E. L. M., Chai, S.-L., Chen, Y., Colwell, R. K., Chazdon, R. L., Clark, C., Clark, D. B., Clark, D. A., Culmsee, H., Damas, K., Dattaraja, H. S., Dauby, G., Davidar, P., DeWalt, S. J., Doucet, J.-L., Duque, A., Durigan, G., Eichhorn, K. A. O., Eisenlohr, P. V., Eler, E., Ewango, C., Farwig, N., Feeley, K. J., Ferreira, L., Field, R., de Oliveira Filho, A. T., Fletcher, C., Forshed, O., Franco, G., Fredriksson, G., Gillespie, T., Gillet, J.-F., Amarnath, G., Griffith, D. M., Grogan, J., Gunatilleke, N., Harris, D., Harrison, R., Hector, A., Homeier, J., Imai, N., Itoh, A., Jansen, P. A., Joly, C. A., de Jong, B. H. J., Kartawinata, K., Kearsley, E., Kelly, D. L., Kenfack, D., Kessler, M., Kitayama, K., Kooyman, R., Larney, E., Laumonier, Y., Laurance, S., Laurance, W. F., Lawes, M. J., Amaral, I. L. do, Letcher, S. G., Lindsell, J., Lu, X., Mansor, A., Marjokorpi, A., Martin, E. H., Meilby, H., Melo, F. P. L., Metcalfe, D. J., Medjibe, V. P., Metzger, J. P., Millet, J., Mohandass, D., Montero, J. C., de Morisson Valeriano, M., Mugerwa, B., Nagamasu, H., Nilus, R., et al.: An estimate of the number of tropical tree species, *Proc. Natl. Acad. Sci.*, 112, 7472–7477, <https://doi.org/10.1073/pnas.1423147112>, 2015.
- 700 Sotta, E. D., Veldkamp, E., Schwendenmann, L., Guimarães, B. R., Paixão, R. K., Ruivo, M., Lola Da Costa, A. C., and Meir, P.: Effects of an induced drought on soil carbon dioxide (CO₂) efflux and soil CO₂ production in an Eastern Amazonian rainforest, Brazil, 2007.
- Sousa Neto, E., Carmo, J. B., Keller, M., Martins, S. C., Alves, L. F., Vieira, S. A., Piccolo, M. C., Camargo, P., Couto, H. T. Z., Joly, C. A., and Martinelli, L. A.: Soil-atmosphere exchange of nitrous oxide, methane and carbon dioxide in a gradient of elevation in the coastal Brazilian Atlantic forest, *Biogeosciences*, 8, 733–742, <https://doi.org/10.5194/bg-8-733-2011>, 2011.
- 710 Stoffel, M. A., Nakagawa, S., and Schielzeth, H.: partR2: partitioning R² in generalized linear mixed models, *PeerJ*, 9, e11414, <https://doi.org/10.7717/peerj.11414>, 2021.

- Tathy, J. P., Cros, B., Delmas, R. A., Marengo, A., Servant, J., and Labat, M.: Methane emission from flooded forest in central Africa, *J. Geophys. Res. Atmospheres*, 97, 6159–6168, <https://doi.org/10.1029/90JD02555>, 1992.
- 715 Upstill-Goddard, R. C., Salter, M. E., Mann, P. J., Barnes, J., Poulsen, J., Dinga, B., Fiske, G. J., and Holmes, R. M.: The riverine source of CH₄ and N₂O from the Republic of Congo, western Congo Basin, *Biogeosciences*, 14, 2267–2281, <https://doi.org/10.5194/bg-14-2267-2017>, 2017.
- Verchot, L. V., Dannenmann, M., Kengdo, S. K., Njine-Bememba, C. B., Rufino, M. C., Sonwa, D. J., and Tejedor, J.: Land-use change and Biogeochemical controls of soil CO₂, N₂O and CH₄ fluxes in Cameroonian forest landscapes, *J. Integr. Environ. Sci.*, 2020.
- 720 Wanninkhof, R.: Relationship between wind speed and gas exchange over the ocean revisited, *Limnol. Oceanogr. Methods*, 12, 351–362, <https://doi.org/10.4319/lom.2014.12.351>, 2014.
- Werner, C., Kiese, R., and Butterbach-Bahl, K.: Soil-atmosphere exchange of N₂O, CH₄, and CO₂ and controlling environmental factors for tropical rain forest sites in western Kenya, *J. Geophys. Res. Atmospheres*, 112, <https://doi.org/10.1029/2006JD007388>, 2007.
- 725 Werner, R. A. and Brand, W. A.: Referencing strategies and techniques in stable isotope ratio analysis, *Rapid Commun. Mass Spectrom.*, 15, 501–519, <https://doi.org/10.1002/rcm.258>, 2001.
- Werner, R. A., Bruch, B. A., and Brand, W. A.: ConFlo III – an interface for high precision $\delta^{13}\text{C}$ and $\delta^{15}\text{N}$ analysis with an extended dynamic range, *Rapid Commun. Mass Spectrom.*, 13, 1237–1241, [https://doi.org/10.1002/\(SICI\)1097-0231\(19990715\)13:13<1237::AID-RCM633>3.0.CO;2-C](https://doi.org/10.1002/(SICI)1097-0231(19990715)13:13<1237::AID-RCM633>3.0.CO;2-C), 1999.
- 730 Werner, R. A., Rothe, M., and Brand, W. A.: Extraction of CO₂ from air samples for isotopic analysis and limits to ultra high precision $\delta^{18}\text{O}$ determination in CO₂ gas, *Rapid Commun. Mass Spectrom.*, 15, 2152–2167, <https://doi.org/10.1002/rcm.487>, 2001.
- Wickham, H.: *ggplot2*, Springer New York, New York, NY, <https://doi.org/10.1007/978-0-387-98141-3>, 2009.
- 735 Wickham, H., François, R., Henry, L., Müller, K., and Vaughan, D.: *dplyr: A Grammar of Data Manipulation*, R Package Version 1.14, 2023.
- Wild, J., Kopecký, M., Macek, M., Šanda, M., Jankovec, J., and Haase, T.: Climate at ecologically relevant scales: A new temperature and soil moisture logger for long-term microclimate measurement, *Agric. For. Meteorol.*, 268, 40–47, <https://doi.org/10.1016/j.agrformet.2018.12.018>, 2019.
- 740 Zanchi, F. B., Waterloo, M. J., Dolman, A. J., Groenendijk, M., Kesselmeier, J., Kruijt, B., Bolson, M. A., Luizão, F. J., and Manzi, A. O.: Influence of drainage status on soil and water chemistry, litter decomposition and soil respiration in central Amazonian forests on sandy soils, *Ambiente E Agua - Interdiscip. J. Appl. Sci.*, 6, 6–29, <https://doi.org/10.4136/ambi-agua.170>, 2011.